Dielectric solvation dynamics of molecules of arbitrary shape and charge distribution

Xueyu Song and David Chandler
Department of Chemistry, University of California, Berkeley, California 94720

(Received 5 September 1997; accepted 3 November 1997)

A new perspective of dielectric continuum theory is discussed. From this perspective a dynamical generalization of a boundary element algorithm is derived. This generalization is applied to compute the solvation dynamics relaxation function for chromophores in various solvents. Employing quantum chemical estimates of the chromophore's charge distribution, the Richards–Lee estimate of its van der Waals surface, and the measured frequency dependent dielectric constant of the pure solvent, the calculated relaxation functions agree closely with those determined by experiments. © *1998 American Institute of Physics.* [S0021-9606(98)50806-9]

I. INTRODUCTION

This paper describes a generally applicable algorithm for applying dielectric continuum theory and its generalizations to solvation and solvation dynamics with realistic models of solute molecular shape and charge distribution. The algorithm is based on the Gaussian field formulation of traditional dielectric continuum theory.[1] For static applications, our method is closely related to the widely used boundary element method for electrostatic calculations.[2–5] But our method offers a dynamical generalization and possible extension to molecular models of a solvent.

As an application, we give a comparison with recent experimental measurements of solvation relaxation functions for coumarin343$^-$(C343$^-$) in water[6] and coumarin153 (C153) in methanol and acetonitrile.[7] The inputs to our calculations are the charge distribution change of the chromophore from the electronic ground state to its first electronically excited state, the chromophore's molecular surface,[8] and the frequency dependent dielectric constant of the solvent. The first of these is estimated from quantum chemistry calculations; the second is determined from standard atomic van der Waals radii; the third is found from experiments. With these ingredients, good agreement between experiments and theory is found. Other standard approximations(e.g., the dipole in a sphere model, and the uniform dielectric approximation[9]) are shown to be less satisfactory.

We begin with a general relation for the response function of a solvent in the presence of a solute, Eq. (1) below. We derive the connection between this relationship and the boundary element method.[3–5] In Sec. III, we test our methodology for the case of a charge distribution in a spherical dielectric cavity. Kirkwood's analytical result for this case is reproduced. In Sec. IV, we apply our formulation to several experimental systems where the solute is definitely not spherical. The paper is concluded in Sec. V.

II. INTEGRAL EQUATION FORMULATION

In Ref. 1 , the following general relationship is derived

$$\boldsymbol{\chi}^{(\mathrm{m})}(\mathbf{r},\mathbf{r}';s)=\boldsymbol{\chi}(\mathbf{r},\mathbf{r}';s)-\int\int_{\mathrm{in}}d\mathbf{r}''d\mathbf{r}'''\boldsymbol{\chi}(\mathbf{r},\mathbf{r}'';s)\cdot\boldsymbol{\chi}_{\mathrm{in}}^{-1}(\mathbf{r}'',\mathbf{r}''';s)\cdot\boldsymbol{\chi}(\mathbf{r}''',\mathbf{r}';s). \quad (1)$$

Here, $\boldsymbol{\chi}^{(\mathrm{m})}(\mathbf{r},\mathbf{r}';s)$ is the solvent dipole density response function of the solution, and $\boldsymbol{\chi}(\mathbf{r},\mathbf{r}';s)$ is that same quantity, but for the pure solvent. The dipole density is a vector. Hence, $\boldsymbol{\chi}^{(\mathrm{m})}(\mathbf{r},\mathbf{r}';s)$ and $\boldsymbol{\chi}(\mathbf{r},\mathbf{r}';s)$ are 3×3 matrices. The ''in'' labeling the integration symbol means the integration is limited to the region occupied by the solute and from which the solvent dipole density is expelled. The inverse of the ''in'' matrix, $\boldsymbol{\chi}_{\mathrm{in}}^{-1}(\mathbf{r},\mathbf{r}';s)$, is defined as

$$\int_{\mathrm{in}}d\mathbf{r}''\boldsymbol{\chi}_{\mathrm{in}}^{-1}(\mathbf{r},\mathbf{r}'';s)\cdot\boldsymbol{\chi}_{\mathrm{in}}(\mathbf{r}'',\mathbf{r}';s)=\delta(\mathbf{r}-\mathbf{r}')\mathbf{I}, \quad (2)$$

where $\mathbf{I}$ is the 3×3 identity matrix associated with the Cartesian coordinates of a three-dimensional system, and $\boldsymbol{\chi}_{\mathrm{in}}(\mathbf{r},\mathbf{r}';s)$ is $\boldsymbol{\chi}(\mathbf{r},\mathbf{r}';s)$ when both $\mathbf{r}$ and $\mathbf{r}'$ are within the ''in'' region, and it is zero otherwise.

In dielectric continuum theory, the response function is[1,10]

$$\boldsymbol{\chi}(\mathbf{r},\mathbf{r}';s)=\frac{\varepsilon(s)-1}{4\pi\varepsilon(s)}\left[\varepsilon(s)\,\delta(\mathbf{r}-\mathbf{r}')\mathbf{I}-\frac{\varepsilon(s)-1}{4\pi}\nabla\nabla'\frac{1}{|\mathbf{r}-\mathbf{r}'|}\right], \quad (3)$$

where $\varepsilon(s)$ is dielectric constant as a function of frequency, s. Assuming

$$\boldsymbol{\chi}_{\mathrm{in}}^{-1}(\mathbf{r},\mathbf{r}';s)=\frac{4\pi\varepsilon(s)}{\varepsilon(s)-1}\left[\frac{1}{\varepsilon(s)}\,\delta(\mathbf{r}-\mathbf{r}')\mathbf{I}+\frac{\varepsilon(s)-1}{4\pi\varepsilon(s)}\nabla\nabla'\,\frac{1}{|\mathbf{r}-\mathbf{r}'|}+\nabla\nabla' f(\mathbf{r},\mathbf{r}';s)\right],\tag{4}$$

we can find an equation for $f(\mathbf{r},\mathbf{r}';s)$ after adopting a specific form for $\boldsymbol{\chi}(\mathbf{r},\mathbf{r}';s)$. By using the dielectric continuum form, Eq. (3), Eq. (2) gives

$$\varepsilon(s)f(\mathbf{r},\mathbf{r}';s)+\frac{(\varepsilon(s)-1)^2}{4\pi\varepsilon(s)}\,\frac{1}{|\mathbf{r}-\mathbf{r}'|}-\left(\frac{\varepsilon(s)-1}{4\pi}\right)^2\frac{1}{\varepsilon(s)}\int_{\mathrm{in}}d\mathbf{r}''\,\nabla''\frac{1}{|\mathbf{r}-\mathbf{r}''|}\cdot\nabla''\frac{1}{|\mathbf{r}''-\mathbf{r}'|}-\frac{\varepsilon(s)-1}{4\pi}\int_{\mathrm{in}}d\mathbf{r}''\,\nabla''f(\mathbf{r},\mathbf{r}'';s)\cdot\nabla''\frac{1}{|\mathbf{r}''-\mathbf{r}'|}=0.\tag{5}$$

This result is an integral equation for the short ranged function $f(\mathbf{r},\mathbf{r}';s)$. To simplify this last equation, the volume integration can be converted to a surface integral. In particular, if $\mathbf{r}$ is within the ‘‘in’’ region, and if $\mathbf{r}'=\mathbf{R_0}$ is on the surface, S, surrounding the ‘‘in’’ region, then $f(\mathbf{r},\mathbf{R_0};s)$ satisfies

$$\frac{\varepsilon(s)+1}{2}f(\mathbf{r},\mathbf{R_0};s)-\frac{\varepsilon(s)-1}{4\pi}\oint_S da_{\mathbf{R}}\;f(\mathbf{r},\mathbf{R};s)\nabla_{\mathrm{n}}\frac{1}{|\mathbf{R}-\mathbf{R_0}|}-\left(\frac{\varepsilon(s)-1}{4\pi}\right)^2\frac{1}{\varepsilon(s)}\oint_S da_{\mathbf{R}}\frac{1}{|\mathbf{R}-\mathbf{R_0}|}\nabla_{\mathrm{n}}\frac{1}{|\mathbf{R}-\mathbf{r}|}=0.\tag{6}$$

Here, $da_{\mathbf{R}}$ is the normal area element at position $\mathbf{R}$ of the surface S and ∇_{n} stands for the outward normal gradient at $\mathbf{R}$. This equation is derived using Green's first identity[11]. Once $f(\mathbf{R},\mathbf{R};s)$ is solved from above equation, the short ranged $f(\mathbf{r},\mathbf{r}';s)$ for both $\mathbf{r}$ and $\mathbf{r}'$ within the ‘‘in’’ region is obtained from

$$f(\mathbf{r},\mathbf{r}';s)=\frac{\varepsilon(s)-1}{4\pi}\oint_S da_{\mathbf{R}}\;f(\mathbf{r},\mathbf{R})\nabla_{\mathrm{n}}\frac{1}{|\mathbf{R}-\mathbf{r}'|}+\left(\frac{\varepsilon(s)-1}{4\pi}\right)^2\frac{1}{\varepsilon(s)}\oint_S da_{\mathbf{R}}\frac{1}{|\mathbf{R}-\mathbf{r}'|}\nabla_{\mathrm{n}}\frac{1}{|\mathbf{R}-\mathbf{r}|}.\tag{7}$$

The calculation of $\boldsymbol{\chi}_{\mathrm{in}}^{-1}(\mathbf{r},\mathbf{r}';s)$ is thus reduced to a two-dimensional integral equation, Eq. (6). In general, an analytical solution to Eq. (6) is difficult to find. Except for some special geometries, such as a spherical cavity, we need to solve the equation numerically. One numerical method of solution is discussed in Sec. IV. Once we solve Eq. (6), the response function of the system can be calculated from Eqs. (4), (7) and (1) and all the properties of the system can be calculated from it through linear response theory.

For example, consider a charge distribution created at time $t=0$ inside a dielectric cavity. The Fourier transform of the time dependent solvation energy of the charge distribution due to the dielectric is[1]

$$E(s)=\frac{1}{s}\sum_{\mathbf{r_i},\mathbf{r_j}}\int\int d\mathbf{r}d\mathbf{r}'\nabla\frac{q_i}{|\mathbf{r}-\mathbf{r_i}|}\cdot\boldsymbol{\chi}^{(\mathrm{m})}(\mathbf{r},\mathbf{r}';s)\cdot\nabla'\frac{q_j}{|\mathbf{r}'-\mathbf{r_j}|},\tag{8}$$

where $\mathbf{r_i}$ is the position of the ith charge, q_i. As shown in Appendix A, this equation for $E(s)$ can be reduced through the application of Eqs. (1) and (4), giving

$$E(s)=-\frac{1}{s}\,\frac{4\pi\varepsilon(s)}{\varepsilon(s)-1}\sum_{\mathbf{r_i},\mathbf{r_j}}q_i\,q_j\,f(\mathbf{r_i},\mathbf{r_j};s).\tag{9}$$

This equation is one of our major results. It relates the calculation of the time dependent non-equilibrium solvation energy to that of a short ranged non-singular function. With Eqs. (6) and (7), the result is a time dependent generalization of the boundary element method for performing dielectric continuum calculations. This connection can be seen by considering

$$\sigma(\mathbf{r},\mathbf{R};s)=\nabla_{\mathrm{n}}f(\mathbf{r},\mathbf{R};s)+\frac{\varepsilon(s)-1}{4\pi\varepsilon(s)}\nabla_{\mathrm{n}}\frac{1}{|\mathbf{r}-\mathbf{R}|}.\tag{10}$$

In Appendix B, it is shown that $\sigma(\mathbf{r},\mathbf{R};s)$ satisfies the following integral equation:

$$\sigma(\mathbf{r},\mathbf{R_0};s)-\frac{\varepsilon(s)-1}{\varepsilon(s)+1}\,\frac{1}{2\pi}\oint_S da_{\mathbf{R}}\sigma(\mathbf{r},\mathbf{R};s)\nabla_{\mathrm{n}}\frac{1}{|\mathbf{R}-\mathbf{R_0}|}-\frac{\varepsilon(s)-1}{\varepsilon(s)+1}\,\frac{1}{2\pi}\nabla_{\mathrm{n}_0}\frac{1}{|\mathbf{r}-\mathbf{R_0}|}=0,\tag{11}$$

where ∇_{n_0} denotes the outward normal gradient at $\mathbf{R_0}$ and the solvation energy can be expressed in terms of $\sigma(\mathbf{r},\mathbf{R};s)$,

$$E(s)=-\frac{1}{s}\sum_{\mathbf{r_i},\mathbf{r_j}}\oint_S da_{\mathbf{R}}\;q_i\sigma(\mathbf{r_i},\mathbf{R};s)\frac{q_j}{|\mathbf{R}-\mathbf{r_j}|}.\tag{12}$$

When comparing with the boundary element method,[3–5] we can identify $\sigma(\mathbf{r},\mathbf{R};s)$ as the induced charge at $\mathbf{R}$. Equation (29) in Ref. 3b is equivalent to our Eq. (11).

In general, the formulation of this section is not confined to the continuum theory of a non-ionic dielectric. For example, in place of Eq. (3), one may use a response function matrix appropriate to a homogeneous ionic solution. A short length scale with molecular detail could also be included. Equation (4) could be written, but the resulting integral equation for $f(\mathbf{r},\mathbf{r}';s)$ will be modified due to the features in $\boldsymbol{\chi}(\mathbf{r},\mathbf{r}';s)$ referring to ionic strength and molecular detail. For the applications given in this paper, however, we confine ourselves to the case of a non-ionic dielectric continuum solvent.

III. SPHERICAL CAVITY

For a spherical cavity, Eq. (6) can be solved analytically. On expanding the f function in spherical harmonics $Y_{lm}(\theta,\phi)$ for a spherical cavity with radius R,

$$f(\mathbf{r},\mathbf{r}';s)=\sum_{lm} B_l(r,r';s)Y^*_{lm}(\theta,\phi)Y_{lm}(\theta',\phi'), \tag{13}$$

where r, θ and ϕ are spherical coordinates of $\mathbf{r}$. Substitution into Eq. (6) yields

$$B_l(r,R;s)=-\frac{(\varepsilon(s)-1)^2}{\varepsilon(s)}\frac{l+1}{2l+1}\frac{1}{(l+1)\varepsilon(s)+l}\frac{r^l}{R^{l+1}}. \tag{14}$$

Combining Eq. (14) with Eq. (7) gives

$$B_l(r,r';s)=-\frac{(\varepsilon(s)-1)^2}{\varepsilon(s)}\frac{l+1}{2l+1}\frac{1}{(l+1)\varepsilon(s)+l}\frac{(rr')^l}{R^{2l+1}}. \tag{15}$$

We use this result to calculate solvation energy of a charge distribution inside a spherical dielectric cavity. In particular, from Eq. (9), the solvation energy for a unit charge at position $\mathbf{b}$ in this cavity is

$$E(s)=\frac{1}{sR}\left(1-\frac{1}{\varepsilon(s)}\right)\sum_l \frac{(l+1)\varepsilon(s)}{(l+1)\varepsilon(s)+l}\left(\frac{b}{R}\right)^{2l}. \tag{16}$$

This equation is precisely the Kirkwood result obtained by solving the Poisson equation,[12] but generalized to the frequency dependent case.

The exact solvation energy, Eq. (16), can be compared with that obtained from the *uniform* dielectric approximation (UDA). In the UDA, the solvation energy of a unit charge at position $\mathbf{b}$ in a dielectric cavity is

$$E_{\mathrm{UDA}}(s)=\frac{1}{s}\int\int_{\mathrm{out}} d\mathbf{r}d\mathbf{r}'\nabla\frac{1}{|\mathbf{r}-\mathbf{b}|}\cdot\boldsymbol{\chi}(\mathbf{r},\mathbf{r}';s)\cdot\nabla'\frac{1}{|\mathbf{r}'-\mathbf{b}|}, \tag{17}$$

where the integration limit ''out'' indicates the integration over $\mathbf{r},\mathbf{r}'$ outside the solute dielectric cavity. For a spherical cavity, the integration can be done analytically, giving

$$E_{\mathrm{UDA}}(s)=\frac{1}{sR}\left(1-\frac{1}{\varepsilon(s)}\right)\times\sum_l\frac{(l+1)(l+1+l\varepsilon(s))}{(2l+1)^2}\left(\frac{b}{R}\right)^{2l}. \tag{18}$$

From these expressions, the solvation relaxation function,[6]

$$S(t)=\frac{\tilde{E}(t)-\tilde{E}(\infty)}{\tilde{E}(0)-\tilde{E}(\infty)}, \tag{19}$$

can be calculated. Here, $\tilde{E}(t)$ is the inverse Fourier transform of $E(s)$ at time t. The results of the calculation are shown in Fig. 1. It is seen that UDA is in serious error if the charge is near the dielectric cavity surface. The exact results show that a general distribution of charges can induce a range of relaxation times.

IV. NUMERICAL SOLUTION AND COMPARISON WITH EXPERIMENTS

We now discuss how to solve the integral Eq. (11) numerically and combine it with Eq. (12) to calculate the time dependent solvation energy of a charge distribution inside a dielectric cavity. To demonstrate our algorithm we first calculate the solvation energy of a charge distribution inside a spherical cavity, where the analytical solution is known [Eq. (16)]. Then the numerical algorithm is applied to three ex-

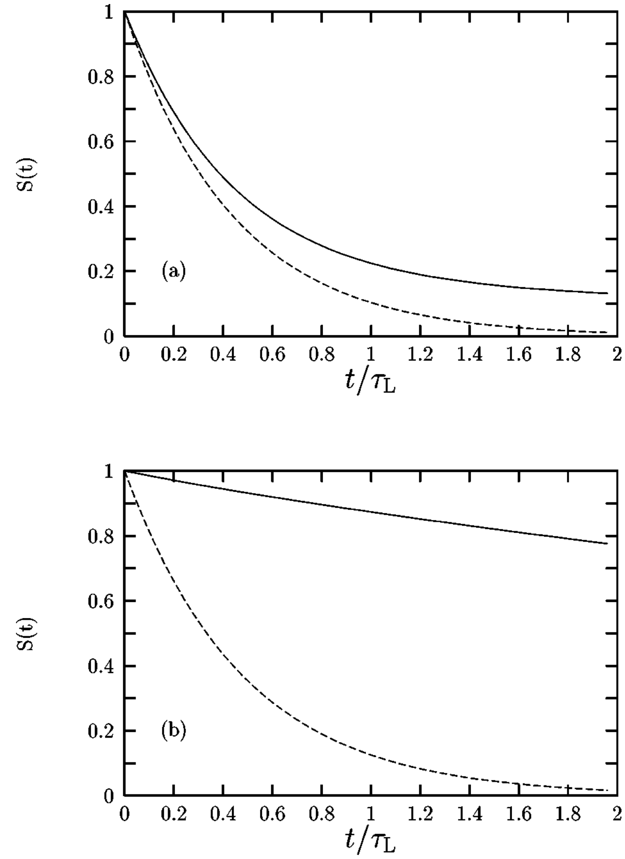

FIG. 1. Solvation relaxation function, $S(t)$, calculated from the exact result [from Eq. (16), dashed line] and the UDA [from Eq. (18), solid line]. The frequency dependent Debye dielectric constant, $\varepsilon(s)=\varepsilon_\infty+(\varepsilon_0-\varepsilon_\infty)/(1-is\tau_D)$ with $\varepsilon_\infty=4.21$ and $\varepsilon_0=78.3$, is used in the calculation. Time t is scaled by the longitudinal relaxation time, $\tau_L=\tau_D(2\varepsilon_\infty+1)/(2\varepsilon_0)$. Panel (a) is for a charge located at 0.5 Å from the center of a sphercal cavity with 10 Å radius. Panel (b) is for a charge being at 7.5 Å from the origin.

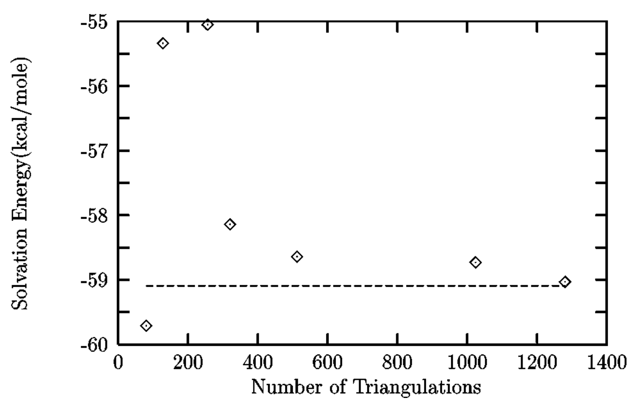

FIG. 2. The convergence test of our numerical algorithm for the solvation energy as a function of number of triangulations. The test system has the following charge distribution: a unit charge at (−8.0,0.0,0.0), a two unit charge at (8.0,0.0,0.0) and a negtive two unit charge at (8.0,1.0,0.0), all inside a spherical cavity of a radius 10 Å centered at the origin. The dielectric constant of the outside dielectric (i.e., the solvent) is 80. The line is the exact result from Eq. (16) and the data points are from numerical calculation.

TABLE I. The atomic charge distribution of C343^{-}.[a]

Serial No.	Atom Type	Coordinates	of	Atoms	Ground state charge	Δq[b]
1	C	−2.4435	−0.7162	0.0020	0.4650	−0.1637
2	C	−2.4544	0.7162	−0.0020	−0.3904	0.2170
3	C	−1.2309	1.4098	0.0083	−0.0804	−0.2205
4	C	0.0091	0.7442	0.0093	−0.2430	0.1234
5	C	0.0040	−0.6854	0.0128	0.5457	−0.0432
6	C	−1.2129	−1.4372	0.0285	−0.5457	0.0123
7	C	1.3004	1.4343	0.0066	−0.0186	−0.0133
8	C	2.4699	0.7429	0.0020	−0.4094	0.0929
9	C	2.4280	−0.7429	−0.0020	1.0397	−0.1000
10	O	1.1736	−1.3659	0.0018	−0.6026	0.0154
11	N	−3.6715	−1.4159	−0.0300	−0.7079	0.0278
12	C	−3.7359	1.5115	−0.0016	0.3132	−0.0943
13	H	−1.2378	2.5030	0.0117	0.1672	−0.0122
14	H	1.2883	2.5255	0.0089	0.1383	0.0155
15	C	3.8519	1.4606	0.0013	0.9237	−0.0192
16	O	3.3349	−1.5637	−0.0098	−0.6377	0.0380
17	C	−1.1784	−2.9468	0.0568	0.3867	−0.0263
18	O	4.3389	1.7387	−1.1213	−0.9745	0.0346
19	O	4.3463	1.7272	1.1235	−0.9742	0.0357
20	C	−4.9493	−0.7309	0.1723	0.4280	−0.0072
21	C	−3.7209	−2.8669	−0.2230	0.4731	0.0343
22	C	−4.9672	0.6936	−0.4070	−0.1131	0.0327
23	C	−2.5243	−3.5931	0.4102	−0.1208	0.0289
24	H	−3.6519	2.3834	−0.6917	−0.0561	0.0221
25	H	−3.8988	1.9444	1.0151	−0.0598	0.0231
26	H	−0.4279	−3.3103	0.7962	−0.0464	−0.0028
27	H	−0.8436	−3.3250	−0.9388	−0.0611	−0.0009
28	H	−5.1916	−0.6991	1.2677	−0.0578	0.0024
29	H	−5.7755	−1.3145	−0.3073	−0.0526	−0.0019
30	H	−3.7718	−3.0949	−1.3203	−0.0691	−0.0063
31	H	−4.6615	−3.2820	0.2197	−0.0681	−0.0148
32	H	−5.0452	0.6496	−1.5174	0.0094	−0.0043
33	H	−5.8922	1.2076	−0.0587	−0.0131	−0.0060
34	H	−2.5310	−4.6537	0.0693	−0.0173	−0.0125
35	H	−2.6491	−3.6309	1.5169	0.0079	−0.0071

[a]The charge distributions given in this table, based upon the procedures noted in the text, were provided by Mark Maroncelli. Similar information for C153 is given in Ref. 17.
[b]Δq—the charge difference, in units of the charge of an electron, between ground state and excited state.

perimental systems. The solvation relaxation function is calculated from the time dependent solvation energy and a direct comparison with experimental results of C343^{-} in water,[6] C153 in methanol and C153 in acetonitrile[7] is made.

The numerical method to solve the integral Eq. (11) over a surface is based on collocation methods by Atkinson and co-workers.[13] Basis functions prescribed in Ref. 13 are set up over the surface by triangulation, and the integral equation is converted to a system of linear equations. In Fig. 2, a convergence test is shown to indicate that good agreement with the analytical result can be obtained with a reasonable number of triangulations over the surface, even for severe situations (e.g., $\varepsilon=80$, and charges located inside but about 2 Å away from the surface of a 10 Å spherical dielectric cavity).

For our solvation dynamics applications, the time dependent solvation energy is obtained by the following procedure: For a molecule like C343^{-}, we use the Lee and Richards molecular surface.[8] Triangulation over this surface is done by Zauhar's method.[14] The probe radius of water is 1.4 Å and the van der Waals radii of the atoms are taken from the CHARMM parameter package.[15] The atomic charge distribution and its change due to electronic excitation of C343^{-} are obtained from electrostatic fits to a semi-empirical modified neglect of differential overlap (MNDO) wave function[16,2] calculated using the AMPAC program package. The resulting partial charges are given in the entrees to Table I. For C153, a similarly derived set of partial charges are tabulated in Ref. 17. The frequency dependent dielectric constant of solvents, $\varepsilon(s)$, are taken from Refs. 19 and 20.

With the above information, the time dependent solvation energy has been calculated by carrying out the inverse Fourier transform of Eq. (12). The results are shown in Figs. 3, 4 and 5. It is clear that all of the major features in experimental results, the initial inertial decay and the multiple exponential long time relaxation, are reproduced almost quantitatively by our calculations. Also shown in Figs. 3, 4 and 5 are the results where a dipole within a spherical cavity is used as a model of the solute.[18] In this simple model, $S(t)$ is the inverse Fourier transform of $(\varepsilon(s)-1)/(2\varepsilon(s)+1)$. It is independent of the dipole magnitude and independent of the cavity size. The comparison between this simple model and our detailed calculations shows that $S(t)$ can be relatively insensitive to the detailed charge distribution and the shape of the probe solute. This insensitivity does not necessarily

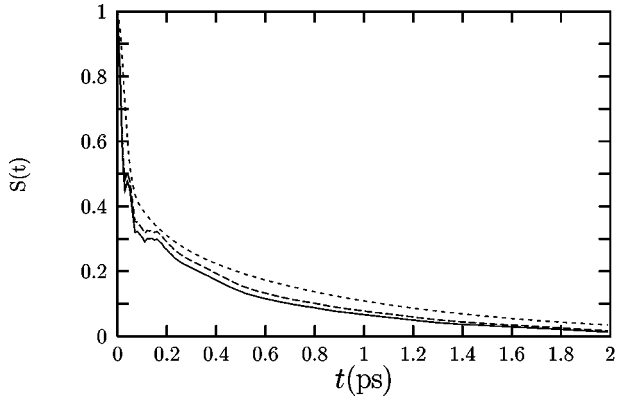

FIG. 3. The comparison of solvation relaxation function between theory and experiments for $C343^{-}$ in water. The short dash curve is from experiments (Ref. 6), the long dash curve is from our calculation, and the solid curve is from a dipole in a spherical cavity model (Ref. 18). The dielectric data are from Ref. 19.

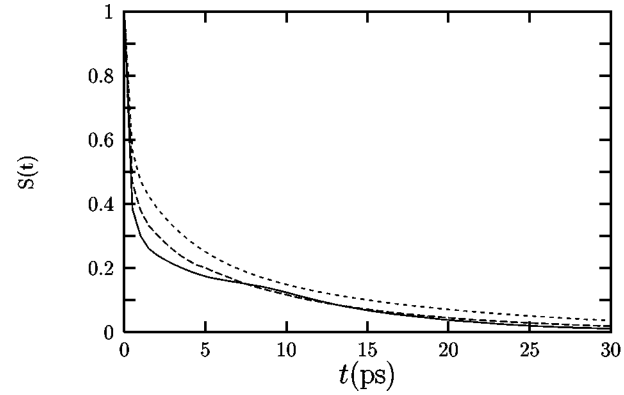

FIG. 5. The comparison of solvation relaxation function between theory and experiments for C153 in methanol. The short dash curve is from experiments (Ref. 7), the long dash curve is from our calculation, and the solid curve is from a dipole in a spherical cavity model. The dielectric data are from Ref. 20.

hold for the absolute size of the solvation energy. For example, the charge distribution change for $C343^{-}$ is about 2.5 D. To reproduce the value of $E(0)$ with this dipole in a spherical cavity, the effective cavity radius would be about 3.7 Å. This radius size seems unphysically small in view of the space filling model of $C343^{-}$ (see Fig. 6).

Equation (11) is linear in $\sigma(\mathbf{r},\mathbf{R};s)$. Therefore, this one equation is to be solved whether there are one, two, or any number of charges. Since solving this equation represents the dominant time consuming step in implementing our approach the solvation energy calculation is almost independent of the numbers of charges inside a dielectric cavity. As the size of the solute increases, the number of triangulations needed to obtain an accurate result increases. For large solutes, this feature can be a major disadvantage of boundary element methods. Some new algorithms have been designed to overcome this disadvantage.[5]

One may use the induced dipole on the dielectric cavity surface to account for the effect of dielectric. We show in Appendix B that the induced dipole method is equivalent to the induced charge scheme. In numerical tests for charge distributions in a spherical cavity, we find that these two methods give the same result with equal triangulations and the computational time is almost the same. Thus, the induced dipole scheme offers no obvious advantages.

V. CONCLUDING REMARKS

In this report we have explored the utility of the Gaussian field theoretic formulation of dielectric continuum theory. With this formulation, we have derived a practical algorithm to calculate time dependent solvation energy for an arbitrary charge distribution in a dielectric cavity with realistic molecular shape. While it has much in common with the well known boundary element method, the formulation generalizes the method so as to treat solvation dynamics. Further, as discussed in Sec. II, it seems possible to extend the method so as to treat the effects of short length scale solvent structure and non-zero ionic strength.

The response of a Gaussian field model is by definition linear. This feature may be a significant limitation of our approach when non-linear response becomes important.[21] It may be possible to describe the effects of non linearities

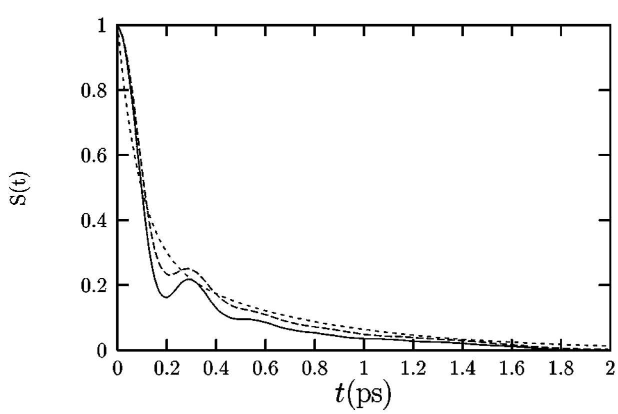

FIG. 4. The comparison of solvation relaxation function between theory and experiments for C153 in acetonitrile. The short dash curve is from experiments (Ref. 7), the long dash curve is from our calculation, and the solid curve is from a dipole in a spherical cavity model. The dielectric data are from Ref. 20.

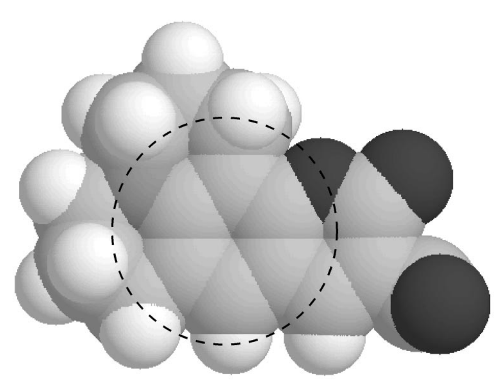

FIG. 6. A space-filling model of $C343^{-}$. The dashed line shows the size of the sphere where the dipole in a spherical cavity model gives the same solvation energy as the full calculation.

through perturbation theory, where a general Gaussian field model serves as a reference. This possibility merits consideration in the future.

ACKNOWLEDGMENTS

This research has been supported by the Basic Energy Science Division of the US Department of Energy. We are indebted to Randy Zauhar for providing us with the triangulation computer program package for determining molecular surfaces. The charge distribution of C343$^-$ and C153 used in the paper are kindly provided by Mark Maroncelli.

APPENDIX: DERIVATION OF EQ. (9)

We focus on a situation where there is *one* charge in a dielectric cavity. The generalization to arbitrary charge distribution is straightforward.

Consider a unit charge at position $\mathbf{a}$ inside a dielectric cavity. Begin with Eq. (1) and define $E=E_0-E_c$, where E_0 is the contribution from the first term of $\boldsymbol{\chi}^{(m)}$ and E_c comes from the contribution of the second term of $\boldsymbol{\chi}^{(m)}$. Using Eq. (3) for $\boldsymbol{\chi}$, we find

$$E_0(s)=\frac{1}{s}\int\int d\mathbf{r}d\mathbf{r}'\nabla\frac{1}{|\mathbf{r}-\mathbf{a}|}\cdot\boldsymbol{\chi}(\mathbf{r},\mathbf{r}';s)\cdot\nabla'\frac{1}{|\mathbf{r}'-\mathbf{a}|}$$
$$=\frac{1}{s}\left(1-\frac{1}{\varepsilon(s)}\right)E_s, \tag{A1}$$

where E_s is the self-energy of a unit charge. Similarly,

$$E_c(s)=\frac{1}{s}\int\int d\mathbf{r}d\mathbf{r}'\nabla\frac{1}{|\mathbf{r}-\mathbf{a}|}$$
$$\cdot\int\int_{\text{in}} d\mathbf{r}''d\mathbf{r}'''\boldsymbol{\chi}(\mathbf{r}-\mathbf{r}'';s)$$
$$\cdot\boldsymbol{\chi}_{\text{in}}^{-1}(\mathbf{r}'',\mathbf{r}''';s)\cdot\boldsymbol{\chi}(\mathbf{r}'''-\mathbf{r}';s)\cdot\nabla'\frac{1}{|\mathbf{r}'-\mathbf{a}|}. \tag{A2}$$

By using Eq. (3) for $\boldsymbol{\chi}$, the integration over $\mathbf{r},\mathbf{r}'$ can be performed, giving

$$E_c(s)=\frac{1}{s}\left(\frac{\varepsilon(s)-1}{4\pi\varepsilon(s)}\right)^2\int\int_{\text{in}} d\mathbf{r}''d\mathbf{r}'''\ \nabla''\frac{1}{|\mathbf{r}''-\mathbf{a}|}$$
$$\cdot\boldsymbol{\chi}_{\text{in}}^{-1}(\mathbf{r}'',\mathbf{r}''';s)\cdot\nabla'''\frac{1}{|\mathbf{r}'''-\mathbf{a}|}. \tag{A3}$$

With Eq. (4), the integration over $\mathbf{r}'',\mathbf{r}'''$ can be done, to yield

$$E_c(s)=\frac{1}{s}\left(1-\frac{1}{\varepsilon(s)}\right)E_s+\frac{1}{s}\frac{4\pi\varepsilon(s)}{\varepsilon(s)-1}f(\mathbf{a},\mathbf{a};s). \tag{A4}$$

Combining Eqs. (A1) and (A4), the self-energy contributions cancel, giving

$$E(s)=-\frac{1}{s}\frac{4\pi\varepsilon(s)}{\varepsilon(s)-1}f(\mathbf{a},\mathbf{a};s). \tag{A5}$$

APPENDIX B: DERIVATION OF EQS. (11) AND (12)

From Eq. (5) we can easily show that $f(\mathbf{r},\mathbf{r}';s)$ satisfies

$$\nabla'^2 f(\mathbf{r},\mathbf{r}';s)=0. \tag{B1}$$

Thus, by Green's theorem[11] we find

$$\oint_S da_{\mathbf{R}}\ f(\mathbf{r},\mathbf{R};s)\nabla_n\frac{1}{|\mathbf{R}-\mathbf{R_0}|}-\oint_S da_{\mathbf{R}}\nabla_n\ f(\mathbf{r},\mathbf{R};s)\frac{1}{|\mathbf{R}-\mathbf{R_0}|}$$
$$=-2\pi f(\mathbf{r},\mathbf{R_0};s), \tag{B2}$$

$$\oint_S da_{\mathbf{R}} f(\mathbf{r},\mathbf{R};s)\nabla_n\frac{1}{|\mathbf{R}-\mathbf{r}'|}-\oint_S da_{\mathbf{R}}\nabla_n\ f(\mathbf{r},\mathbf{R};s)\frac{1}{|\mathbf{R}-\mathbf{r}'|}$$
$$=-4\pi f(\mathbf{r},\mathbf{r}';s). \tag{B3}$$

Combining Eqs. (B2), (6) and (10) with the following identity[22]

$$\nabla_{n_0}\oint_S da_{\mathbf{R}}\ I(\mathbf{r},\mathbf{R};s)\frac{1}{|\mathbf{R}-\mathbf{R_0}|}$$
$$=\oint_S da_{\mathbf{R}} I(\mathbf{r},\mathbf{R};s)\nabla_n\frac{1}{|\mathbf{R}-\mathbf{R_0}|}+2\pi I(\mathbf{r},\mathbf{R_0};s), \tag{B4}$$

where $I(\mathbf{r},\mathbf{R};\mathbf{s})$ is an arbitrary function of $\mathbf{r},\mathbf{R}$ and s, then, Eq. (11) can be obtained.

Equation (12) can be derived from Eqs. (7), (9), (10) and (B3).

Consider

$$p(\mathbf{r},\mathbf{R};s)=f(\mathbf{r},\mathbf{R};s)+\frac{\varepsilon(s)-1}{4\pi\varepsilon(s)}\frac{1}{|\mathbf{r}-\mathbf{R}|}. \tag{B5}$$

With Eq. (6), it can be shown that $p(\mathbf{r},\mathbf{R};s)$ satisfies the following integral equation:

$$p(\mathbf{r},\mathbf{R_0};s)-\frac{\varepsilon(s)-1}{\varepsilon(s)+1}\frac{1}{2\pi}\oint_S da_{\mathbf{R}}\ p(\mathbf{r},\mathbf{R};s)\nabla_n\frac{1}{|\mathbf{R}-\mathbf{R_0}|}$$
$$-\frac{\varepsilon(s)-1}{\varepsilon(s)+1}\frac{1}{2\pi}\frac{1}{|\mathbf{r}-\mathbf{R_0}|}=0, \tag{B6}$$

and the solvation energy can be expressed in terms of $p(\mathbf{r},\mathbf{R};s)$,

$$E(s)=-\frac{1}{s}\sum_{\mathbf{r_i},\mathbf{r_j}}\oint_S da_{\mathbf{R}}\ q_i\ p(\mathbf{r_i},\mathbf{R};s)\nabla_n\frac{q_j}{|\mathbf{R}-\mathbf{r_j}|}. \tag{B7}$$

It is thus clear that $p(\mathbf{r},\mathbf{R};s)$ is the induced dipole in the normal direction of $\mathbf{R}$ due to a unit charge at position $\mathbf{r}$ inside the dielectric cavity since the induced charge, $\sigma(\mathbf{r},\mathbf{R};s)$, is related to the induced dipole $p(\mathbf{r},\mathbf{R};s)$ in the normal direction of $\mathbf{R}$ by $\sigma(\mathbf{r},\mathbf{R};s)=-\nabla_n\ p(\mathbf{r},\mathbf{R};s)$.[11]

[1] X. Song, D. Chandler, and R. A. Marcus, J. Phys. Chem. **100**, 11954 (1996).
[2] J. Tomasi and M. Persico, Chem. Rev. **94**, 2027 (1994).
[3] (a) R. J. Zauhar and R. S. Morgan, J. Mol. Biol. **186**, 815 (1985); (b) R. J. Zauhar and R. S. Morgan, J. Comput. Chem. **9**, 171 (1988).
[4] B. J. Yoon and A. M. Lenhoff, J. Comput. Chem. **11**, 1080 (1990); M. E. Davis and J. A. McCammon, Chem. Rev. **90**, 509 (1990); R. Bharadwaj,

A. Windemuth, S. Sridharan, B. Honig, and A. Nicholls, J. Comput. Chem. **16**, 898 (1995).
[5] L. R. Pratt, G. J. Tawa, G. Hummer, A. E. Garcia, and S. A. Corcelli, Int. J. Quantum Chem. **64**, 121 (1997), and references therein.
[6] R. Jimenez, G. R. Fleming, P. V. Kumar, and M. Maroncelli, Nature (London) **369**, 471 (1994).
[7] M. L. Horng, J. A. Gardecki, A. Papazyan, and M. Maroncelli, J. Phys. Chem. **99**, 17311 (1995).
[8] F. M. Richards, Annu. Rev. Biophys. Bioeng. **6**, 151 (1977); M. L. Connolly, J. Appl. Crystallogr. **16**, 548 (1983).
[9] B. Bagchi and A. Chandra, J. Chem. Phys. **90**, 7338 (1989); L. E. Fried and S. Mukamel, *ibid.* **93**, 932 (1990); F. O. Raineri, Y. Zhou, H. L. Friedman, and G. Stell, Chem. Phys. **152**, 201 (1991).
[10] M. S. Wertheim, Annu. Rev. Phys. Chem. **30**, 471 (1979).
[11] J. D. Jackson, *Classical Electrodynamics*, 2nd ed. (Wiley, New York, 1975).
[12] J. G. Kirkwood, J. Chem. Phys. **2**, 341 (1934).
[13] K. Atkinson, SIAM (Soc. Ind. Appl. Math.) J. Sci. Stat. Comput. **15**, 1087 (1994).
[14] R. J. Zauhar, J. Comp-Aided Mol. Des. **9**, 149 (1995); R. J. Zauhar and A. Varnek, J. Comput. Chem. **17**, 864 (1996).
[15] B. R. Brooks, R. E. Bruccoleri, B. D. Olafson, D. J. States, S. Swaminathan, and M. Karplus, J. Comput. Chem. **4**, 187 (1983).
[16] F. A. Momany, J. Phys. Chem. **82**, 592 (1978).
[17] P. V. Kumar and M. Maroncelli, J. Chem. Phys. **103**, 3038 (1995).
[18] C. Hsu, X. Song, and R. A. Marcus, J. Phys. Chem. **101**, 2546 (1997).
[19] X. Song and R. A. Marcus, J. Chem. Phys. **99**, 7768 (1993).
[20] C. Hsu and R. A. Marcus (unpublished).
[21] T. Fonseca and B. M. Landanyi, J. Phys. Chem. **95**, 2116 (1991); M. S. Skaf and B. M. Landanyi, *ibid.* **100**, 18258 (1996); M. Maroncelli and G. R. Fleming, J. Chem. Phys. **89**, 5044 (1988); M. Maroncelli, *ibid.* **94**, 2048 (1991).
[22] M. A. Jaswon and G. T. Symm, *Integral Equation Methods in Potential Theory and Electrostatics* (Academic, London, 1977).